Liquid Crystals
Publication details, including instructions for authors and subscription information:
http://www.informaworld.com/smpp/title~content=t713926090

Computer modelling and simulations of thermotropic and lyotropic alkyl glycoside bilayers

Teoh Teow Chong[a]; Thorsten Heidelberg[a]; Rauzah Hashim[a]; Saadullah Gary[a]
[a] Chemistry Department, Faculty of Science, University of Malaya, 50603 Kuala Lumpur, Malaysia

To cite this Article Chong, Teoh Teow , Heidelberg, Thorsten , Hashim, Rauzah and Gary, Saadullah(2007) 'Computer modelling and simulations of thermotropic and lyotropic alkyl glycoside bilayers', Liquid Crystals, 34: 3, 349 — 363
To link to this Article: DOI: 10.1080/02678290601111556
URL: http://dx.doi.org/10.1080/02678290601111556

Liquid Crystals, Vol. 34, No. 3, March 2007, 349–363

Taylor & Francis
Taylor & Francis Group

Computer modelling and simulations of thermotropic and lyotropic alkyl glycoside bilayers

TEOH TEOW CHONG, THORSTEN HEIDELBERG, RAUZAH HASHIM* and SAADULLAH GARY
Chemistry Department, Faculty of Science, University of Malaya, 50603 Kuala Lumpur, Malaysia

(*Received 12 April 2006; accepted 4 October 2006*)

Simulations on bilayers have previously proven their ability to provide insights to membrane functions such as fusion. Most simulations are based on the major components of cell membranes, which are phospholipids and cholesterol. Membranes can be explained on the basis of hydrophilic and hydrophobic interactions via hydrogen bonding, van der Waals interactions and repulsive forces. While particularly phospholipids have gained significant attention in bio-related modelling and simulations, glycolipids, which constitute another major component of cell membranes, have not been similarly studied. Here we present the simulation of bilayers for the six most common and simple stereoisomeric glycolipids, namely the α- and β-octyl glycosides of glucose, galactose and mannose, in both thermotropic and lyotropic systems. All these compounds form thermotropic smectic A phases and can exhibit lyotropic lamellar assemblies. We have studied the hydrogen bonding and linked the results to the temperature stability of the corresponding liquid crystal phase. In addition to the mesophase-stabilizing effect of hydrogen bonding in general, we found that the thermal stability appears to be particularly affected by intralayer hydrogen bonding. The simulations also confirmed a significant difference in the density of the lipophilic region for α- and β-glycosides, which has previously been used to explain differences in clearing temperatures.

1. Introduction

Alkyl glycosides are simple glycolipids that have proven useful tools in biology and chemistry, due to their ability to act as non-ionic surfactants. For example, commercially available alkyl glucosides [1] have been applied to stabilize, reconstitute, purify and crystallize membrane proteins and membrane-associated protein complexes without denaturation. Besides their simple surfactant applications [2], especially as emulsifiers, alkyl glycosides can also form liposome-like vesicles, thus providing a potential target for drug carriers [3, 4]. In this study the three most simple and common alkyl glycosides, viz. octyl glucopyranoside (C_8Glc), octyl galactopyranoside (C_8Gal) and octyl mannopyranoside (C_8Man), are investigated in both α- and β-anomeric form. These compounds differ only in the stereochemical orientation (axial or equatorial) of the hydroxyl groups at C-2 and C-4 and the alkoxy substituent at C-1 of the sugar unit (figure 1). All of them, as far as they have been analysed (β-C_8Man and α-C_8Gal remain uninvestigated), show thermotropic smectic and lyotropic lamellar phases at low to moderate water concentrations [5]. Despite their structural similarity, the glycosides significantly vary in their transition temperatures. β-C_8Gal, for example, exhibits a smectic A phase at higher temperature (96–127°C) than β-C_8Glc (69–107°C). [5]

In an attempt to understand the variable clearing temperatures for stereoisomeric alkyl glycosides, we have applied computer simulations to bilayer structures for the above mentioned six glycosides. Glycolipid bilayer structures are based on a microphase separation of two incompatible molecular regions, the hydrophilic sugar part and the hydrophobic alkyl chain [6]. With respect to the number of hydroxyl groups in the investigated molecules, and owing to their significantly higher bonding energy contribution compared with other intermolecular interactions, hydrogen bonds are believed to dominate the self-assembly of glycolipids, thus forming the major driving force for liquid crystal phases. We therefore analysed the hydrogen bonding patterns in the pure state and in the presence of water (lyotropic system) and attempted to correlate simulation results with published experimental clearing points.

There have been several previous simulations on bilayers, performed by researchers such as van Buuren and Berendsen [7], Feller *et al.* [8] and Bogusz *et al.* [9]. Particularly interesting is the simulation of a membrane fusion by Ohta-lino *et al.* [10]. However, no evaluation

*Corresponding author. Email: rauzah@um.edu.my

Liquid Crystals
ISSN 0267-8292 print/ISSN 1366-5855 online © 2007 Taylor & Francis
http://www.tandf.co.uk/journals
DOI: 10.1080/02678290601111556

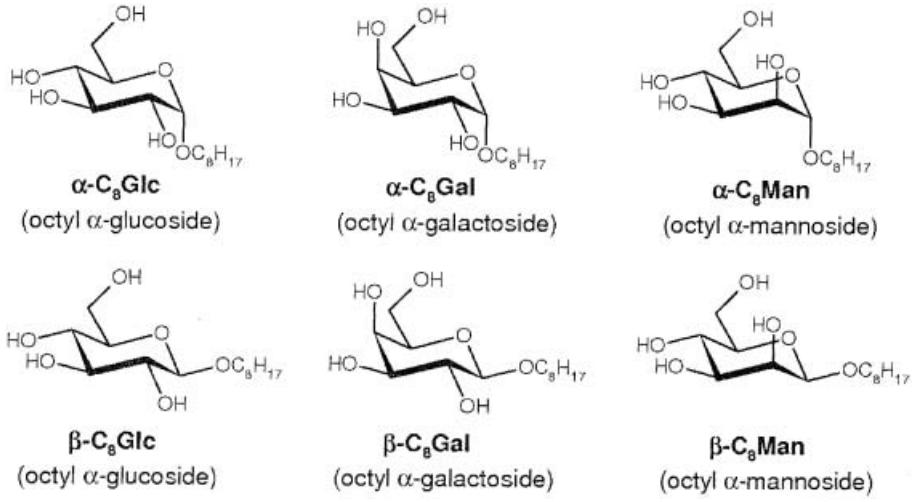

Figure 1. Chemical structures of the investigated glycosides.

of hydrogen bonding, such as the one in this study, has yet been carried out, due to the extensive requirements of computational resources for the simulation. Besides the hydrogen bonding analysis, we have also evaluated the bilayer spacings and local density profiles (LDPs). The density of the lipophilic region has been associated with the stability of glycolipids liquid crystals [5]. In order to evaluate this proposal, we determined this density and correlated it with experimental clearing temperatures.

2. Methods

For each simulation 400 glycolipid molecules were arranged in two bilayers. Firstly a monolayer comprising 10×10 parallel oriented glycolipids was built, based on a cubic lattice pattern, using the Hyperchem crystal builder. In accordance with recent findings [11], the alkyl tails of the glycosides are tilted towards the bilayer axis. Two monolayers were combined, alky tail to alkyl tail, to form the initial bilayer. This configuration was minimized in Hyperchem, to avoid breaking of the aggregation during the final simulation, and subsequently converted into PDB-format using Babel. The final minimization and the molecular dynamic runs were performed on Amber 7 [12] for a set of two of the bilayers. In the case of lyotropic systems, 550 water molecules were arranged on the top and at the bottom of each of the bilayers. This corresponds to a glycolipid concentration of about 85%. The temperature was set at 300 K and all simulations were carried out under constant pressure (NpT) in a cuboid periodic box. An equilibration time of 600 ps was applied with gradual decrease of group harmonic constraint force from 500 to 0 kcal mol^{-1} $Å^{-1}$, followed by a production time of 5 ns in 1 fs steps. Various computer facilities were used, but typically these were provided by UM CAD-CAM Geranium CRAY cluster, comprising 16 nodes, in the Engineering Faculty of the University of Malaya. A 1 ns simulation took about 24 hours to complete.

Hydrogen bonding analyses were performed for every ps. Qualified OH-O hydrogen bonding were selected based on an O–O distance of 4 Å and an angle cutoff of 60°. This criterion is based on the Amber7 manual [12] recommendation of 3.5 Å (we increased the value to 4.0 Å) and 120° in ptraj, corresponding to 4.0 Å and 60° in carnal (figure 2). Hydrogen bonding was classified into three types for the thermotropic and one additional type for lyotropic systems. The first separation differentiated between intramolecular and intermolecular hydrogen bonding; see figures 3 (*c*) and 3 (*b*) The latter were further split into intralayer and interlayer interactions, figure 3 (*a*) [13]. This differentiation reflects the anisotropy of the layer structure and correlates with expected energy differences for the cohesion of molecules within the same layer with respect to those belonging to different layers. Finally for lyotropic systems there remain interactions of sugar and water or solvent–solute hydrogen bonding, figure 3 (*d*).

Bilayer spacing was measured as the distance of the centres of mass for the first and second bilayers, as shown in figure 4 (*a*) The values analysed in this way are the averages based on all 5 000 frames, recorded over the 5 ns simulation period. Alternatively the bilayer spacing was determined from a one-dimensional local density profile (LDP), figure 4 (*b*). The latter approach avoids possible (minor) errors based on *X*- and *Y*-participation to the normally exclusively *Z*-based bilayer distance. This can happen if the centre of mass in the bilayer plane differs slightly for the two bilayers.

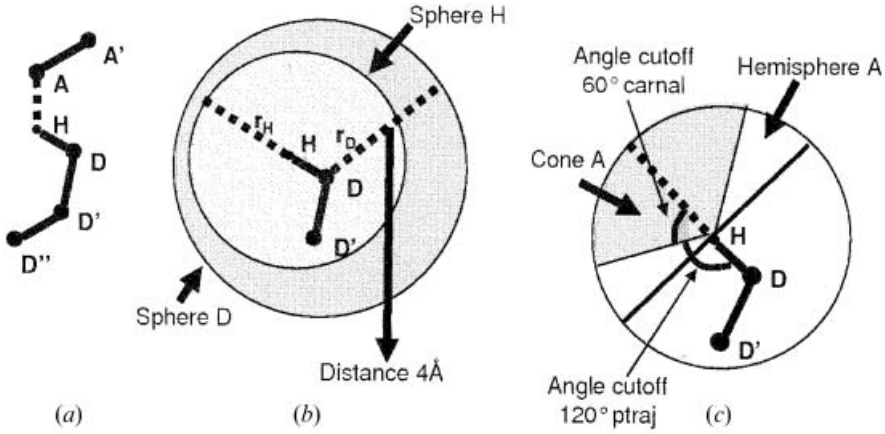

Figure 2. Hydrogen bonding selection criteria. (*a*) Spatial model of a hydrogen bonding interaction (A=hydrogen acceptor, electron pair donor, D–H=hydrogen donor); (*b*) hydrogen bonding selection spheres; (*c*) angle restriction for hydrogen bonding.

However, the LDP-based analysis could only be applied on single simulation frames and, therefore, is more limited with respect to precision. To avoid a systematic error due to a possible expansion or contraction of the bilayers over the simulation time, we evaluated the LDP for one frame each from the start and at the end of the simulation and applied the average. The error estimation considers statistical deviations as well as the limited accuracy of the applied method. The latter we estimated to ± 1 Å, based on 0.5–1 Å intervals applied on simulation-derived coordinates to determine the local density profiles.

The density of the lipid tail was estimated from the mass divided by volume in g cm^{-3}. The volume of the lipid tail was estimated by the HyperChem™ v6.0 Quantitative Structure Activity Relationships

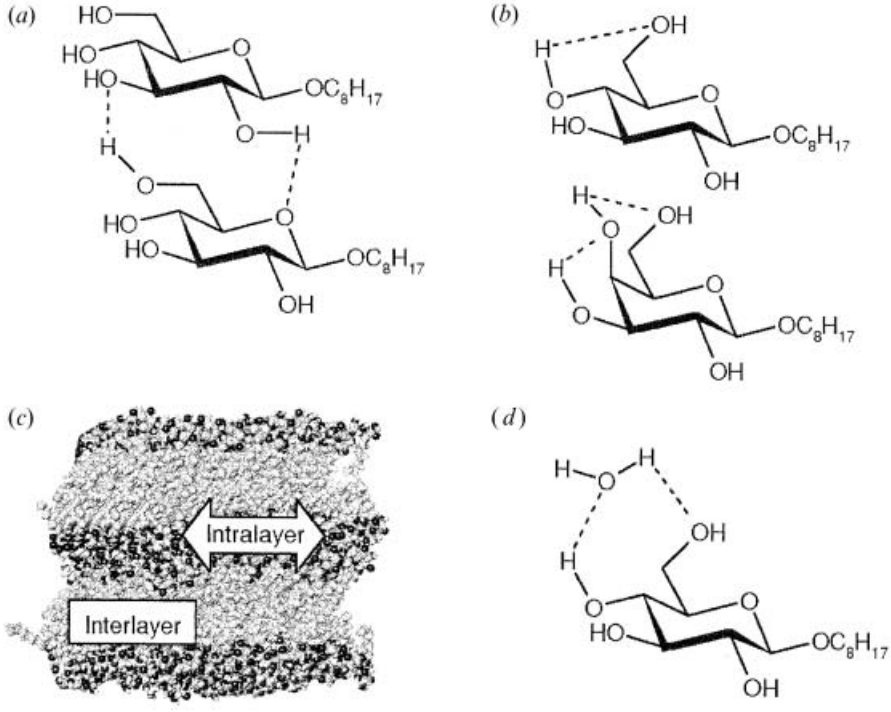

Figure 3. Classification of hydrogen bonding (dotted lines). (*a*) Intermolecular hydrogen bonding; (*b*) intramolecular hydrogen bonding; (*c*) illustration of inter- and intra-layer hydrogen bonding (black=oxygen, grey=carbon, white=hydrogen); (*d*) solvent–lipid hydrogen bonding.

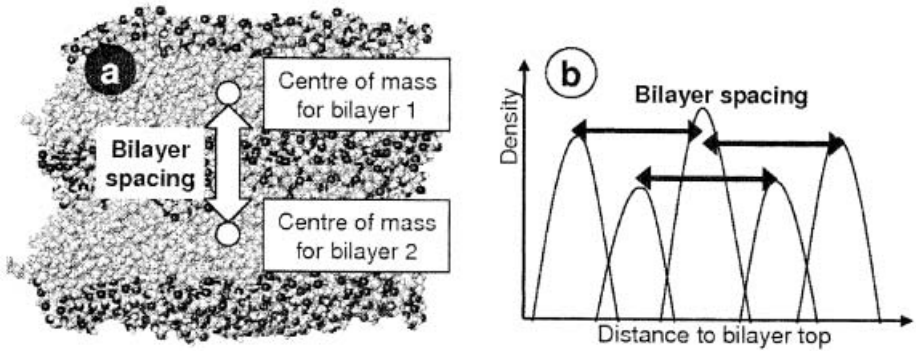

Figure 4. Determination of bilayer spacing. (*a*) Centre of mass approach; (*b*) local density profile approach.

Properties (QSAR Properties) module [14]. Internal surface areas between the hydrophilic and the hydrophobic regions of the glycosides were estimated based on the dimensions of the periodic box along the bilayer. Box dimensions were determined for each nanosecond and averaged over the 5 ns simulation period.

The clearing temperature was estimated using the relationship between energy and temperature derived from the Boltzmann equation. We assume that the main energy stabilizing the bilayer is based on hydrogen bonding and that all the hydrogen bonds are statistically equivalent in energy. Thus, to a good approximation the energy differences in the following equations may be replaced by the hydrogen bonding values. Assuming that the difference in internal energy between the smectic (or the lamellar lyotropic) and the isotropic phase is the same for two stereoisomeric glycosides, e.g. β-C_8Glc and β-C_8Gal, we obtain the following equations based on the Boltzmann equation for internal energy, $E \propto k_B T$ where k_B=Boltzmann constant and T=temperature in Kelvin.

$$\frac{\Delta E_{\beta C_8 Gal}}{\Delta E_{\beta C_8 Glc}} = \frac{k_B T_{\beta C_8 Gal}}{k_B T_{\beta C_8 Glc}}$$
$$T_{\beta C_8 Gal} = \frac{\Delta E_{\beta C_8 Gal}}{\Delta E_{\beta C_8 Glc}} T_{\beta C_8 Gal}. \quad (1)$$

The clearing point for β-C_8Gal, $T_{\beta C_8 Gal}$, can therefore be estimated based on the reference clearing point for β-C_8Glc, $T_{\beta C_8 Glc}$. With respect to neglected energy contributions of factors other than hydrogen bonding, equation (1) should be limited to closely related structures only. Thus, we used separate correlations for α- and β-glycosides.

Based on the uncertainties of the hydrogen bonding we can also estimate the error for the predicted clearing temperature T_c as

$$\sigma T_{\beta C_8 Gal} = \left\{ \left(\frac{T_{\beta C_8 Glc}}{\Delta E_{\beta C_8 Glc}} \sigma(\Delta E_{\beta C_8 Gal}) \right)^2 + \left(\frac{T_{\beta C_8 Glc}(\Delta E_{\beta C_8 Gal})}{(\Delta E_{\beta C_8 Glc})^2} \sigma(\Delta E_{\beta C_8 Glc}) \right)^2 \right\}^{\frac{1}{2}}$$

$\sigma T_{\beta C_8 Gal}$ is the standard deviation for clearing temperature for β-C_8Gal based on β-C_8Glc.

3. Results

3.1. *Hydrogen bonding and clearing temperature, T_c, in thermotropic systems*

Our simulations reveal a significantly higher number of total inter-glycoside hydrogen bonds for α-glycosides than for the β-analogues. While the values per molecule indicate a small but noticeable effect of the sugar configuration for α-glycosides (table 1), β-C_8Glc and β-C_8Gal show identical results (both 3.5 ± 0.1). However, the intralayer hydrogen bonding for the galactoside (2.9 ± 0.1) is significantly higher than for the glucoside (2.7 ± 0.1). Since the intralayer hydrogen bonding is remarkably higher than the interlayer hydrogen bonding, we suggest that the higher clearing point for β-C_8Gal must be due to the higher intralayer hydrogen bonding. Thus, the correlation of clearing temperatures based on equation (1) applies these values instead of the total hydrogen bonding for β-glycosides.

Since intramolecular hydrogen bonds cannot be related to molecular cohesion, we did not primarily focus on them. However, the extent of intramolecular hydrogen bonding can affect intermolecular hydrogen bonding due to the competition of both for hydrogen atoms. Thus, intramolecular hydrogen bonding may indirectly be correlated with bilayer stability. In order to evaluate this possibility, we compared the values for the

Table 1. Intermolecular hydrogen bonding analysis for thermotropic bilayers: T_c calculation based on equation (1).

	α-Man	α-Gal	α-Glc	β-Gal	β-Glc	β-Man
H-bonding						
total	3.96 ± 0.03	3.85 ± 0.04	3.8 ± 0.1	3.5 ± 0.1	3.5 ± 0.1	3.14 ± 0.04
intra-layer	2.61 ± 0.02 (=66%)	2.43 ± 0.04 (=63%)	2.77 ± 0.03 (=73%)	2.9 ± 0.1 (=82%)	2.7 ± 0.1 (=77%)	3.08 ± 0.03 (=98%)
inter-layer	1.35 ± 0.01 (=34%)	1.42 ± 0.003 (=37%)	1.0 ± 0.1 (=27%)	0.64 ± 0.02 (=18%)	0.81 ± 0.03 (=23%)	0.61 ± 0.01 (=2%)
T_c/°C						
experimental	132 [5] 134 [14]	–	116 [5] 118 [14]	127 [5] 133 [14]	107 [5] 108 [14]	–
calculated[a,c]	132 ± 12	121 ± 12	reference	–	–	–
calculated[b,d]	–	–	–	107 ± 15	reference	68 ± 5
calculated[b,c]	–	–	–	135 ± 21	reference	160 ± 17

[a]Ref. α-C_8Glc 116°C. [b]Ref. β-C_8Glc 107°C. [c]Total H-bonding. [d]Intra-layer H-bonding.

β-glycoside series. The data (table 2) indicate no effect for sugar epimers. Assuming this trend to be valid also for the α-series, we conclud, that intramolecular hydrogen bonding may be ignored for this investigation.

Taking α-C_8Glc as reference (T_c=116°C), the calculated clearing temperature of α-C_8Man exactly matches the literature reported value of 132°C. The predicted value for α-C_8Gal of 121°C lies between the gluco- and the galacto-side. For β-C_8Gal, we estimated T_c as 135°C (based on 107°C for β-C_8Glc), which again is in good agreement with experimental values ranging from 127°C [5] to 133°C [15]. The prediction for β-C_8Man depends on the choice of either total interglycoside hydrogen bonding or just intralayer hydrogen bonding (table 1) and will be discussed later.

3.2. *Hydrogen bonding in lyotropic systems*

In lyotropic systems all interglycoside hydrogen bonding is decreased with respect to the thermotropic analogues. However, the impact of water on interlayer hydrogen bonding is, as expected, significantly higher than for intralayer interaction. While the latter suffered only a moderate decrease up to 30%, the former are almost reduced to zero in the case of β-glycosides. For α-glycosides, however, interlayer (interglycoside) hydrogen bonding still remains a considerable cohesion factor. The descending order for total hydrogen bonding in lyotropic system differs from the thermotropic order only in the position of the α-glucoside (tables 1 and 3). An explanation for this behaviour is given in § 4.

Table 2. Intramolecular hydrogen bonding.

β-Gal	β-Man	β-Glc
1.5 ± 0.5	1.5 ± 0.4	1.5 ± 0.4

Clearing temperatures for lyotropic systems are much less easy to compare than for thermotropic analogues, since the data depend on the concentration. Unfortunately, the experimental data for different glycosides, and our simulations, do not reflect the same concentration. Due to this systematic error the potential accuracy of predictions is low, and a qualitative analysis appears more appropriate. As shown in table 3, the sequence of clearing points follows the sequence of the total hydrogen bonding. A slightly more extensive analysis follows in § 4.

3.3. *Local density profile and bilayer spacing*

The local density profiles (LDPs) for all simulations are displayed in figures 5 and 6. We observed only minor differences for frames at the beginning and at the end of the simulation, therefore only one profile for each simulation is given. All LDPs show the expected microphase separation, exhibiting antipodal maxima and minima for the hydrophilic and hydrophobic regions of the glycolipids. In lyotropic systems the density profile of water basically follows that of the hydrophilic head group. However, for β-glycosides we note the occurrence of a water-enriched domain that clearly separates two polar glycolipid regions. α-Glycosides on the other hand hardly show this kind of behaviour.

Table 3. Intermolecular hydrogen bonding analysis for lyotropic bilayers. T_c calculation based on equation (1).

	α-Glc	α-Man	α-Gal	β-Gal	β-Glc	β-Man
H-bonding						
Inter-lipid						
total	2.5 ± 0.1	2.3 ± 0.1	2.3 ± 0.1	2.7 ± 0.1	2.5 ± 0.1	2.9 ± 0.1
intra-layer	2.23 ± 0.03	2.0 ± 0.1	2.03 ± 0.03	2.6 ± 0.1	2.4 ± 0.1	2.88 ± 0.03
$\Delta_{aq\text{-}pure}$	−8%	−18%	−28%	−10%	−11%	−6%
inter-layer	0.24 ± 0.03	0.31 ± 0.04	0.30 ± 0.04	0.06 ± 0.02	0.06 ± 0.03	0
$\Delta_{aq\text{-}pure}$	−82%	−78%	−70%	−90%	−93%	−100%
Solvent-solute						
total	3.7 ± 0.3	3.7 ± 0.2	3.6 ± 0.1	3.0 ± 0.1	3.1 ± 0.2	2.5 ± 0.1
water H-donor	2.4 ± 0.1	2.7 ± 0.1	2.7 ± 0.1	2.3 ± 0.03	2.3 ± 0.1	1.9 ± 0.1
water acceptor	1.3 ± 0.2	1.0 ± 0.1	0.90 ± 0.03	0.7 ± 0.1	0.8 ± 0.1	0.58 ± 0.02
Total	6.2 ± 0.4	6.0 ± 0.3	5.9 ± 0.2	5.7 ± 0.4	5.6 ± 0.3	5.4 ± 0.2
T_c/°C						
experimental	–	140 [5] (6% aq)	–	136 [5] (13% aq)	122 [5] (19% aq)	–
calculated	164 ± 37	150 ± 31	143 ± 26	129 ± 36	reference	108 ± 25

Values for experimental and simulated bilayer spacing are summarized in table 4. β-Glycosides show significantly larger bilayer spacing than α-anomers. This applies both for thermotropic systems as well as for lyotropic analogues, where the bilayer spacing is increased to about 20% for β-glycosides and to 25–30% for α-anomers. While the simulations are in good agreement with SAXS-determined data [5] for thermotropic systems of α-glycosides, the corresponding values for β-compounds exceed experimental data by nearly 10%. Lyotropic simulations overshoot experimental data by about 15%. The two methods used for the determination of the bilayer spacing show no variations for β-glycosides, but differ slightly for the α-anomers, where LDP values are higher than with the centres of mass approach. Interestingly the LDP-derived bilayer spacing proved more accurate for thermotropic systems, while the centres of mass-based method was better for lyotropic systems.

3.4. *Internal microphase surface area and density of the hydrophobic tail region*

Internal microphase surface area and the density of the hydrophobic tail region are interlinked properties, and should be examined in conjunction. The data are summarized in table 5. Our internal surface area per lipid for β-C_8Glc (41 Å^2) significantly exceeds the 38 Å^2 previously reported by Bugusz *et al.* [9]. Considering the lower concentration of water applied in their simulation and our range of values for different β-glycosides, we consider the values to be in reasonable agreement.

In thermotropic systems α-glycosides clearly show higher surface areas and lower densities than β-anomers. However, a different picture results for the lyotropic systems. While the densities for the hydrophobic region are almost unaffected by the presence of water, the size of the interphase changes significantly. Moreover α-glycosides display an inverse behaviour to β-anomers. The latter swell due to absorption of water, whereas the former seem to shrink. For the water concentration applied in our simulations (15%) β-glycosides show higher surface areas than α-glycosides.

4. Discussion

4.1. *Validity of the total hydrogen bonding per lipid*

The maximum number of hydrogen bonds in this study is limited by the availability of suitable protons, unless we accept a proton to be involved in more than one hydrogen bond. For the thermotropic system, the maximum total hydrogen bonding for one lipid is four, based on the four hydroxyl groups. There is also a more stringent constraint related to the availability of donor electron pairs. However, since the number of donors (six oxygen atoms) already exceeds the available protons, this limitation is irrelevant. The simulations determine the total intermolecular hydrogen bonding (excluding intramolecular hydrogen bonding) between 3.1 and 4.0 With our values for intramolecular hydrogen bonding of about 1.5 this adds up to total hydrogen bonding of nearly 5.5.

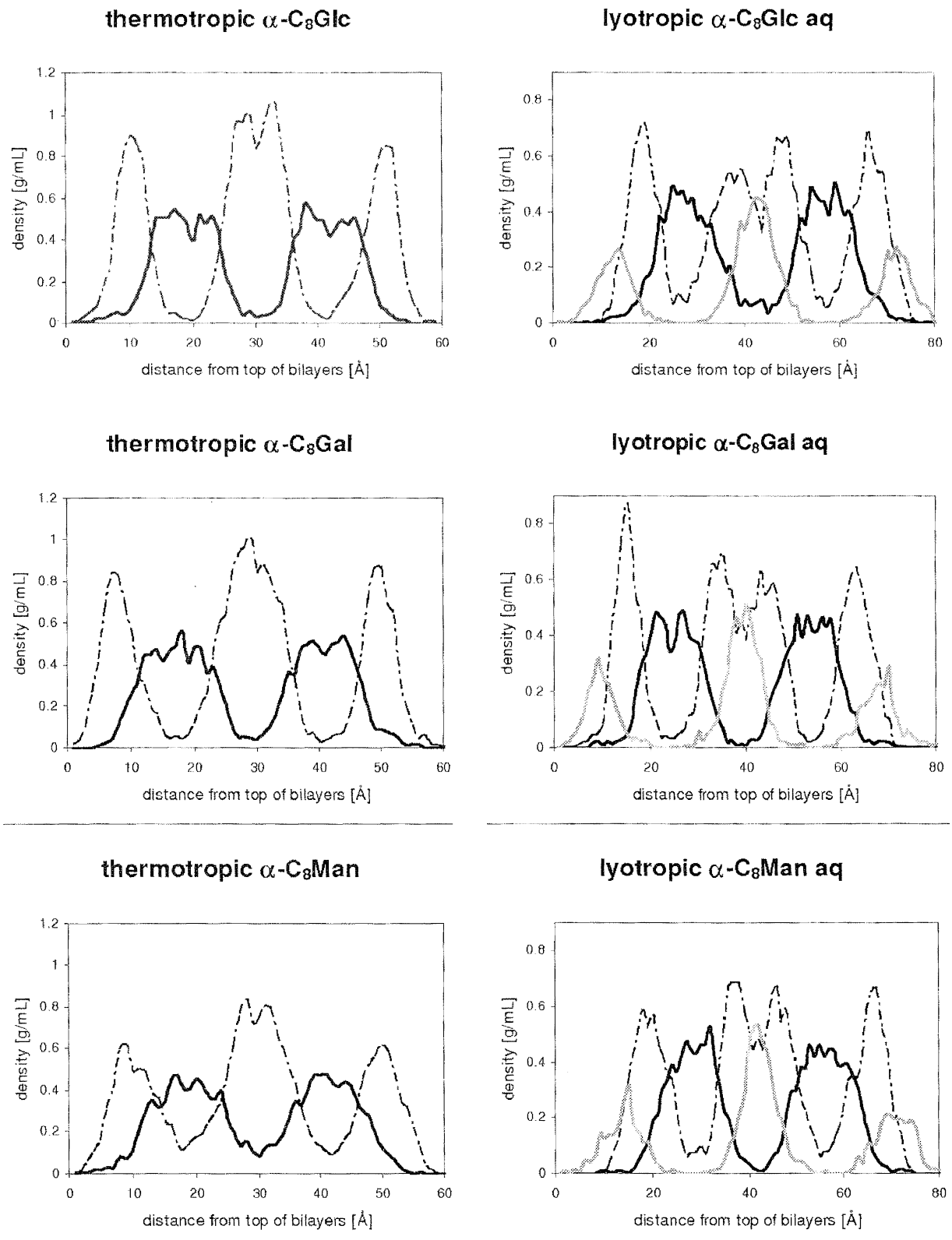

Figure 5. Local density profiles for α-glycosides: (black=alkyl tail, broken=sugar head, grey=solvent=water).

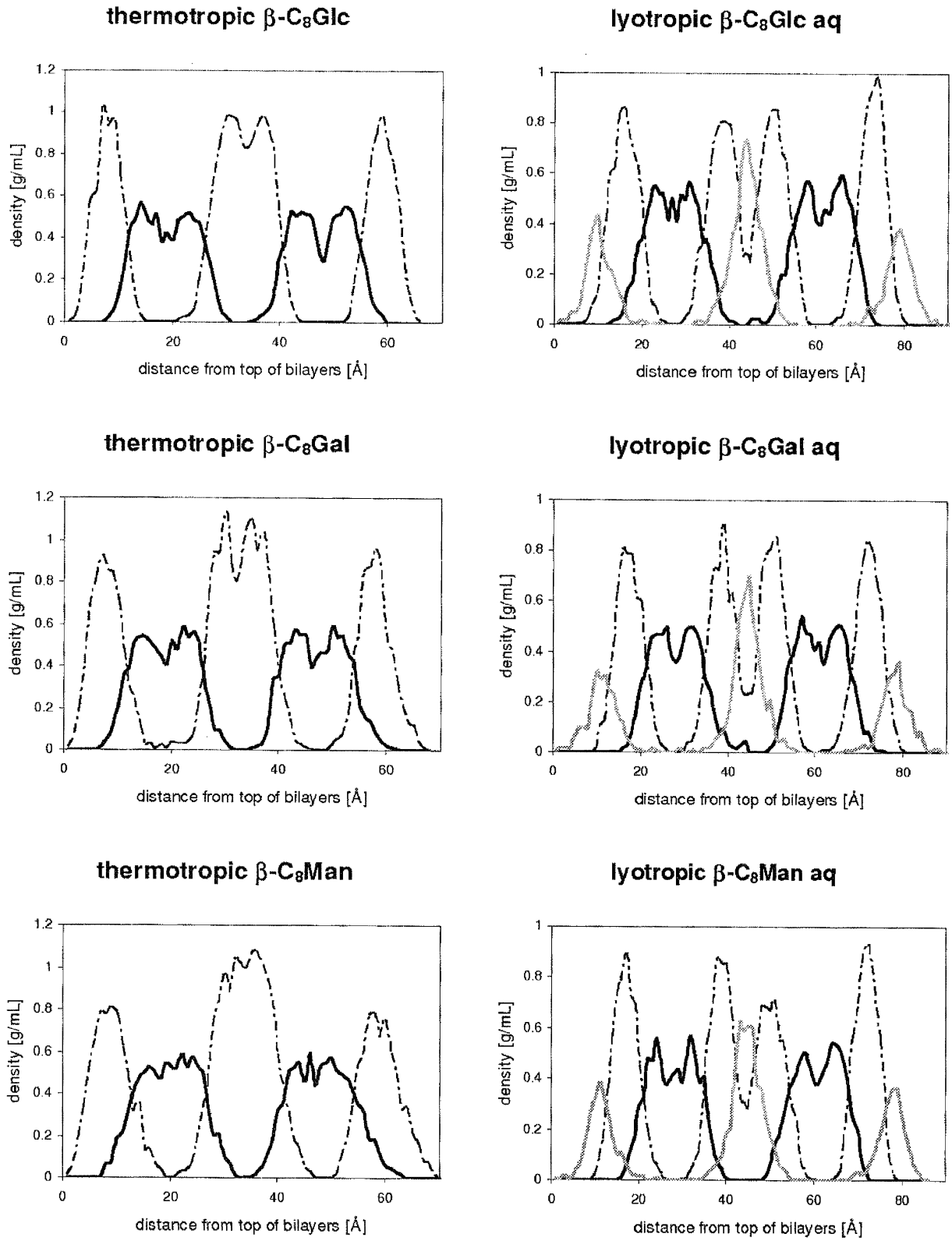

Figure 6. Local density profiles for β-glycosides: (black=alkyl tail, broken=sugar head, grey=solvent=water).

Table 4. Bilayer spacing (Å). COM=centre of mass; LDP=local density profile.

	thermo. bilayer spac.			lyo. bilayer spac.		
Glycoside	COM	LDP	Ref. [5]	COM	LDP	Ref. [5]
α-Glc	21.9±0.1	23±1	23.3	28.5±0.1	29±1	—
α-Gal	22.6±0.2	23±2	—	27.9±0.1	30±2	—
α-Man	20.9±0.3	23±2	23.1	27.4±0.1	29±1	24.3 (6% aq)
β-Glc	28.9±0.1	29±1	25.6	34.62±0.01	35±1	29.7 (19% aq)
β-Gal	28.1±0.1	28±1	25.8	33.2±0.2	34±1	28.2 (15% aq)
β-Man	27.11±0.04	28±2	—	33.2±0.1	33±2	—

The difference of 1.5 is probably due to systematic errors during the hydrogen bonding standard calculation method based on the applied hydrogen bonding selection criteria. Applying the D–A distance instead of D–H–A, where A is the hydrogen acceptor and D is the hydrogen donor [16] (figure 2), increases the range for qualified hydrogen bonding. Also the selection tool does not limit the number of hydrogen bonds for a single hydrogen atom. If several qualified donor centres are found inside a hydrogen atom's qualifying range for hydrogen bonding, then all of them are counted instead of just the nearest or best positioned donor. Thus, our hydrogen bonding calculation is only qualitatively acceptable within the statistical range. This also applies for the lyotropic systems, although our result of 7.7 total hydrogen bonding per glycoside (involving both inter- and intra-molecular interactions) does not exceed the theoretical maximum. The latter is determined as 9.5 due to the availability of suitable hydrogen atoms (4 OH+2.75 water molecules, each worth 2, per glycoside). As stated before for the thermotropic systems, limitations based on acceptor availability do not apply.

4.2. *Validity of local density profiles*

LDPs were determined by single frame analyses only, owing to the extended calculation process. In order to avoid errors based on the modelling dynamics, we compared the LDPs for one frame at the beginning and one at the end of the simulation. Neither LDP showed any significant difference for any of the investigated systems. However, a more accurate approach also requires an examination of intermediate states. We therefore analysed the dynamics of the LDP for each exemplary α- and β-glycoside, taking one frame out of every 1 ns production time (=1000 frames). The results, displayed in figure 7, indicate a steady state system with no significant change. The quasi-static behaviour is even more clearly visible by looking at the LDP-derived bilayer spacings (table 6).

4.3. *Local densities*

The HyperChem™ QSPR tool [14], used for the determination of regional densities, systematically overestimates the density of the hydrophobic region for the applied glycosides. This conclusion results from comparison of the determined values (table 5) with the experimental density for the corresponding hydrocarbon, i.e. octane ($0.8\,g\,ml^{-1}$). While α-glycosides basically seem to maintain the hydrocarbon density, β-anomers exceed this value by about 15%. It is unlikely that such a drastic error derives from the simulation, especially since the corresponding values at the local density profiles, though systematically underestimated themselves, uniformly indicate drastically lower (>30%) densities everywhere inside the alkyl region. Therefore, we conclude that the error must be due to the applied

Table 5. Alkyl tail densities and internal microphase separation surfaces.

	Thermotropic		Lyotropic	
Glycoside	Surface $Å^2$/lipid	Density $g\,ml^{-1}$	Surface $Å^2$/lipid	Density $g\,ml^{-1}$
α-Glc	38.4±0.4	0.82±0.02	35.0±0.4	0.82±0.01
α-Gal	36.6±0.3	0.83±0.02	35.3±0.2	0.82±0.01
α-Man	38.1±0.2	0.83±0.02	36.0±0.4	0.82±0.01
β-Glc	35.8±0.3	0.95±0.01	41.4±1.5	0.95±0.02
β-Gal	35.8±0.3	0.95±0.01	40.3±1.0	0.93±0.01
β-Man	35.3±0.4	0.95±0.01	39.4±1.1	0.94±0.01

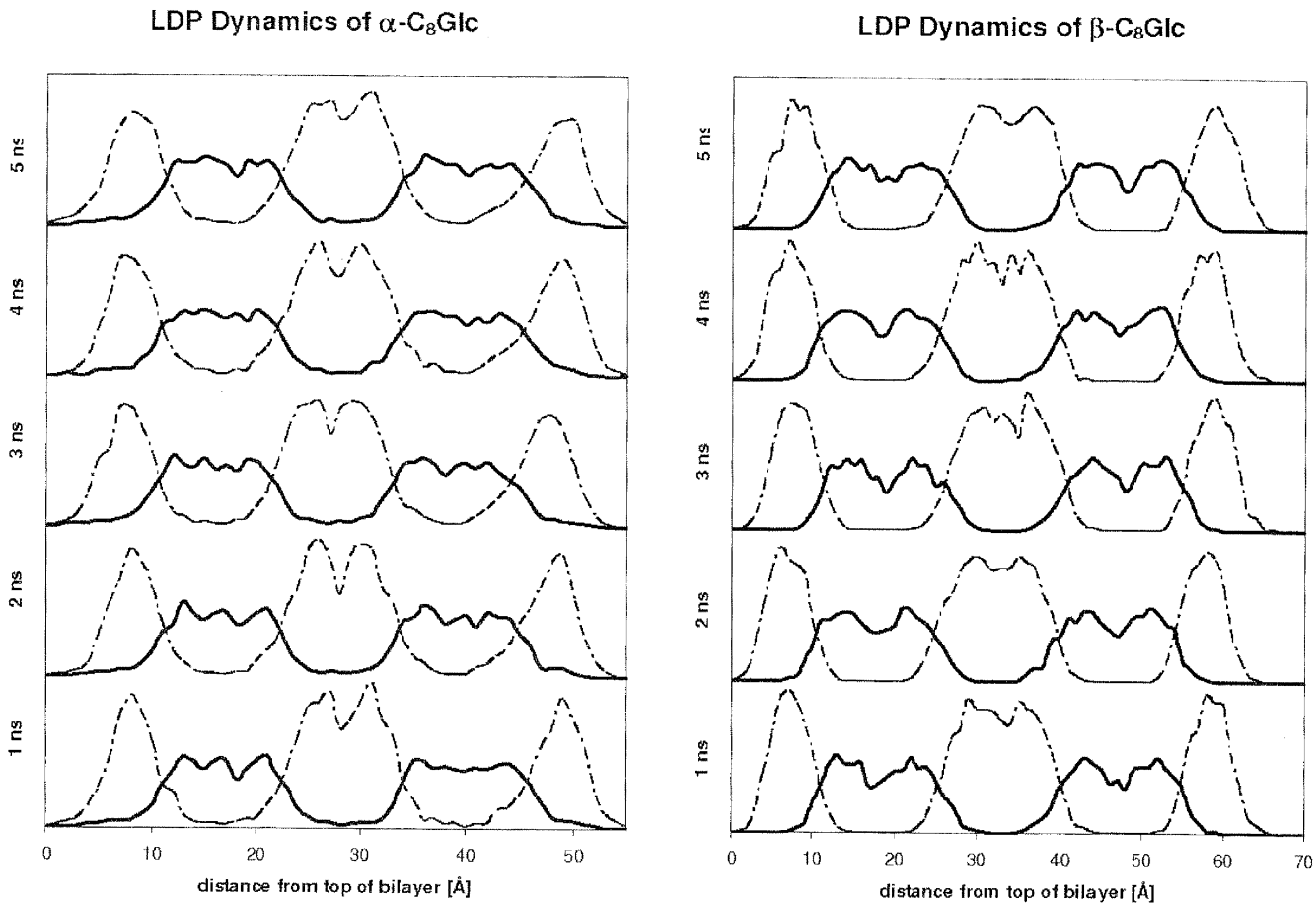

Figure 7. Local density profile dynamics (thermotropic systems): (black=alkyl tail, broken=sugar head).

determination tool. However, a systematic error, while disqualifying the data for direct predictions, does not limit their use for internal comparison.

4.4. *α and β anomers*

Sakya *et al.* have explained differences in clearing points for glycoside anomers based on the internal microphase surface area as a result of the molecular shape of the surfactant [5]. Amphiphilic liquid crystalline assemblies are supposedly driven by hydrogen bonding. Their thermal stability relies on the ability to store energy without disrupting the assembly. According to Sakya most energy will be stored in vibrations of the alkyl chains, due to low limitations based on intermolecular interaction for the hydrophobic region. Larger surface areas permit more vibrations and, therefore, reflect higher clearing points. An analogous explanation correlates lower tail group densities with increased liquid crystal stability. All experimental results so far have indicated higher clearing temperatures for pure α-glycosides than for the corresponding β-anomers. The thermotropic results displayed in table 5 support these findings. An explanation is given in figure 8. The more linear shape of β-glycosides leads to a significantly more dense packing of the alkyl tails than for the bent-shaped α-anomers. However, neither the local tail region density nor the interface area can explain changes in transition temperatures within the α- or β-anomeric groups. Thus the predictive ability for these tools is rather limited.

Table 6. Dynamics of bilayer spacing (Å) based on LDP analysis.

Frame	α-C_8Glc	β-C_8Glc
1 ns	22.5±1.3	29.0±1.4
2 ns	22.8±1.3	28.8±1.5
3 ns	22.5±1.3	29.0±1.4
4 ns	23.0±1.0	28.5±1.3
5 ns	22.8±1.3	29.0±1.4

In lyotropic systems the hydrophobic density and the internal surface area lead to contradicting predictions

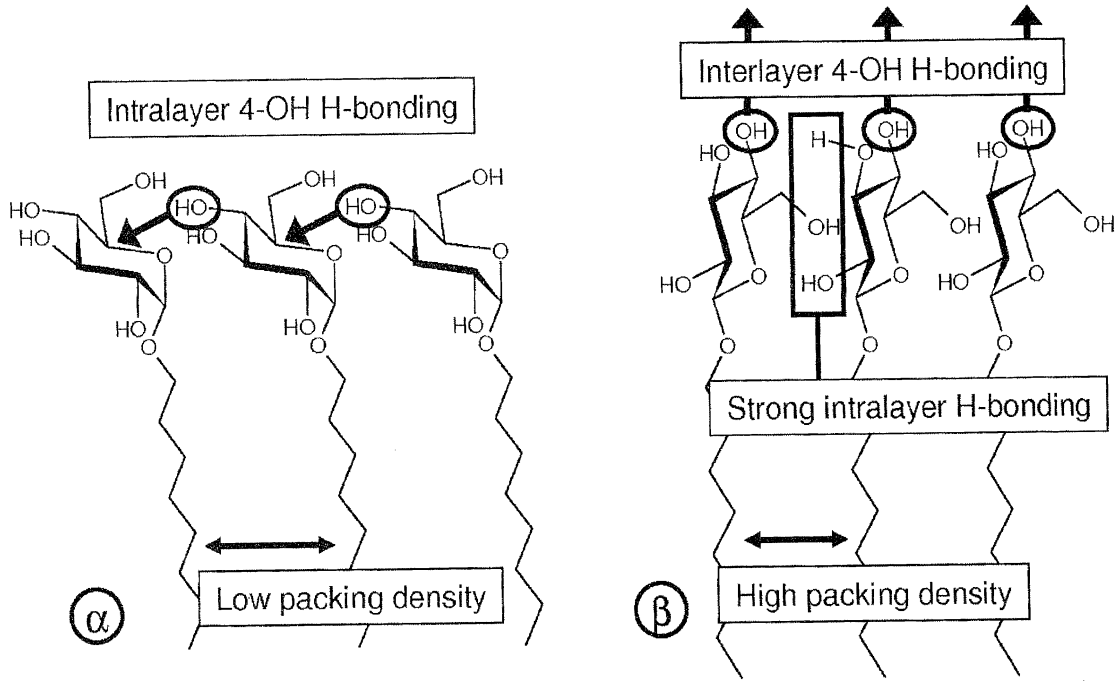

Figure 8. Packing density and hydrogen bonding for α/β-anomeric pairs.

for the clearing temperature of anomers. A significant effect of water on the surface area does not coincide with a change in the density of the alkyl region. In fact the latter is practically unaffected. Since the local tail density is more directly related to vibrational freedom of the glycolipid, we consider this probe more suitable than the surface area. However, limited availability of experimental data and varying concentrations, prevent a proper checking of this prediction tool.

4.5. *Thermotropic systems*

As already stated before, α-glycosides exhibit more hydrogen bonding than β-anomers (table 1). This corresponds to generally higher clearing temperatures for α-compounds, which is in agreement with predictions based on the regional density for the alkyl tail (see above). However, the predictions in table 1 indicate an exception to this behaviour, either for galactose or for mannose, depending on the hydrogen bonding type (total or intralayer) applied in equation (1). With respect to identical total interglycoside hydrogen bonding for β-C_8Glc and β-C_8Gal, we prefer to use intralayer hydrogen bonding for β-glycosides. In this way, the predicted clearing point for the β-galactoside is higher than that for the α-anomer, thus contradicting Sakya's packing oriented theory [5] (see above). Only very few experimental data for clearing points of both galactosides are reported. However, the available data pairs indeed indicate a higher clearing temperature for the β-anomer [17, 18]. We would like to evaluate our intralayer hydrogen bonding-based clearing points for β-glycosides by comparing predictions and experimental data for mannosides. The remarkably different predictions for the clearing point of β-C_8Man, based on either total interglycoside or intralayer hydrogen bonding, provides a good evaluation opportunity. Unfortunately, due to the difficult access of β-mannosides [19], no suitable experimental data are available.

The LDPs indicate local minima at the centres of the alkyl tail region for several glycosides. These minima are especially developed for β-anomers (figure 6) and are believed to originate from a systematic error in our layer arrangement. Due to the effort to minimize vacuum areas inside the simulation box, we arranged the tilted layers facing opposite directions, figure 9 (*a*).

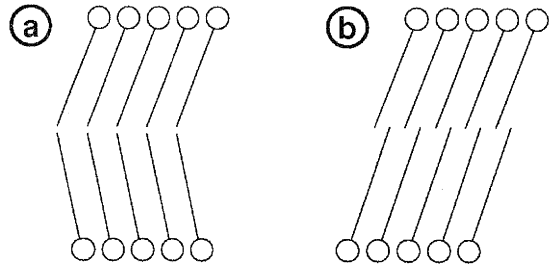

Figure 9. Arrangements of layers for modelling. (*a*) Tilted alkyl chains facing same direction, limited interdigitation; (*b*) antiparallel arrangement of alkyl chains, easy interdigitation of chains.

Unfortunately this arrangement limits the interception of alkyl tails from different layers, thus leading to a central area of lower density. Another impact is a systematic overestimation of the bilayer spacing. The extent of the latter depends on the tilting angle. β-Glycosides are significantly more tilted than α-anomers, therefore it is fitting that our bilayer spacing estimations for α-glycosides are more accurate than for the β-analogues.

In order to evaluate the impact of the layer arrangement on our results, we repeated the simulation of β-C_8Glc using the greater space requirement but easily interceptible parallel arrangement of the tilted tails figure 9 (*b*). However, the simulation output for this arrangement, displayed in figure 10 (*a*), neither significantly changed the shape of the density profile, figure 10 (*b*), nor reduced the bilayer spacing or affected the hydrogen bonding results. Probably the required activation barrier for interlinking the alkyl tails of different layers is too high to be passed during the simulation. This means that an improvement of bilayer predictions will require the full modelling of an interlinked bilayer. Interestingly we determined an analogue LDP minimum for the centre tail region of a previously reported dimyristoyl–glycerol–phosphotidycholine (dmpc) lipid bilayer [20]. The local decrease of density (~25%) matches our findings. With respect to the different extent of the minimum for α- and β-glycosides, we still see this feature as an artefact. However, since our objective is to focus on the stability

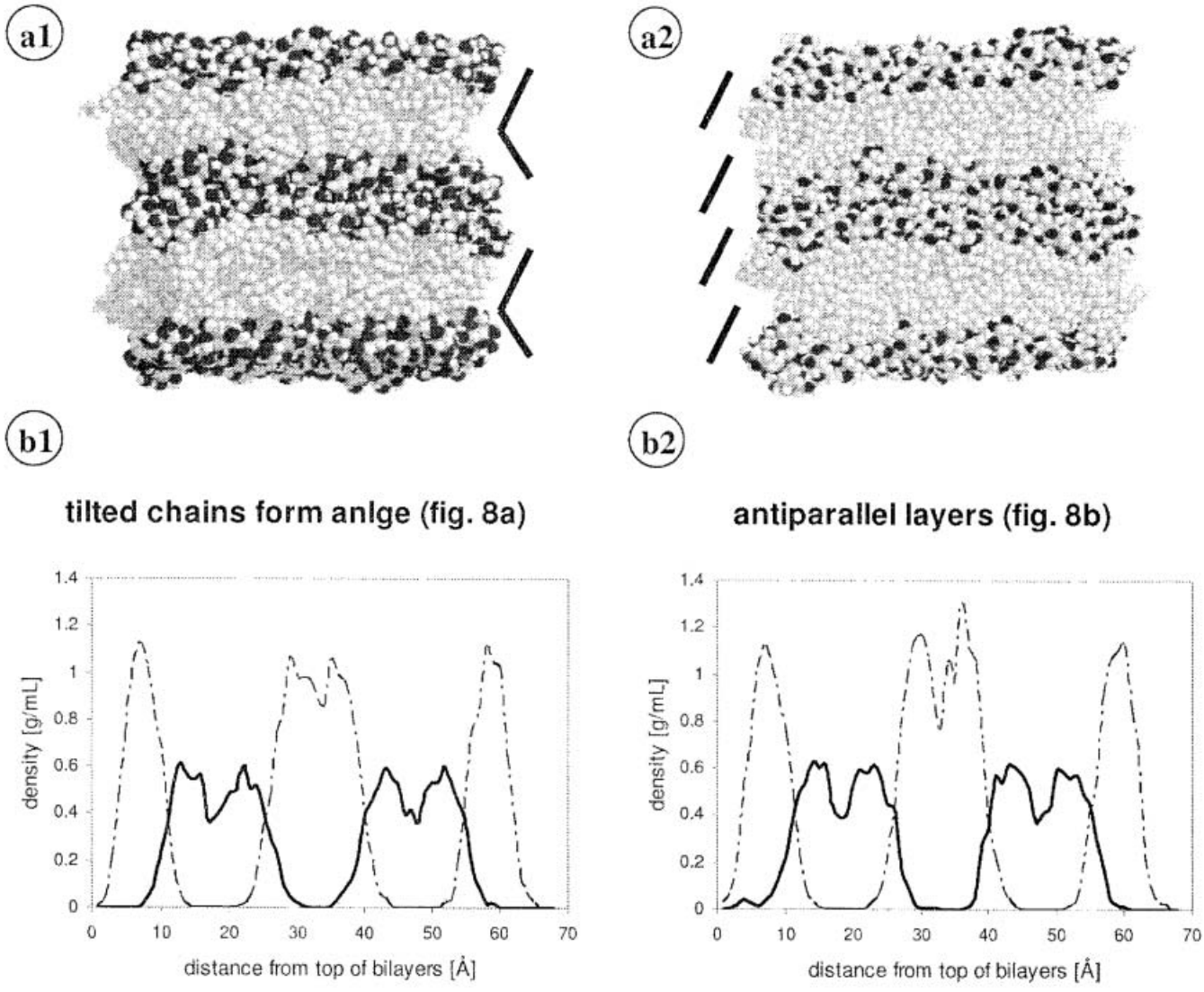

Figure 10. Impact of layer arrangement on simulation output. (*a*) Bilayer arrangement in overview, 1=tilteld arrangement, 2=antiparallel arrangement; (*b*) local density profile.

of bilayer assemblies rather than on their dimensions, we consider such a measure beyond our scope. After all, the hydrogen bonding of the glycolipids is unlikely to be affected by the extent of interdigitation of the alkyl tail region.

Differences for intra- and inter-layer hydrogen bonding of anomeric (α/β) as well as for epimeric pairs (e.g. Glc/Gal) can be explained on the basis of stereochemical arrangements. The linear arrangement of β-glycosides favours intralayer hydrogen bonding (figure 8), while the bent arrangement for α-anomers enhances the opportunity for interlayer hydrogen bonding due to better accessibility of the hydroxyl groups. For β-Glc only the hydroxyl group at C-4 of the sugar really protrudes from the layer and provides reasonable access for interlayer hydrogen bonding. The α-anomer, however, exposes the primary 6-OH, which (due to the methylene spacer between the ring and the hydroxyl group) is more flexibile than secondary OHs. Thus it is not surprising that α-glycosides exhibit higher interlayer hydrogen bonding than β-anomers. Naturally we should expect a reverse trend for the intralayer hydrogen bonding. The data in table 1 show the expected trend. Nonetheless, the extraordinarily low interlayer hydrogen bonding for the mannoside remains surprising.

Figure 11 shows the effect of the stereochemical orientation of a hydroxyl group on its hydrogen bonding preference. The equatorial 4-OH in β-C_8Glc gives rise to interlayer H-bonding, while its axial analogue in β-C_8Gal prefers intralayer interaction. We thus expect more intralayer and less interlayer hydrogen bonding for β-Gal than for β-Glc. Table 1 confirms this expectation. In fact the interlayer hydrogen bonding for β-Gal is likely to rely more on the 3-OH and the 6-OH group. Figure 11 indicates the exposure of the β-C_8Gal 3-OH for interlayer hydrogen bonding. However, since C-3 is embedded deeper inside the layer than C-4, we should expect a lower contribution to interlayer hydrogen bonding compared with an axial 4-OH. For the corresponding α-pair we expect the opposite behaviour. Based on the different hydrogen bonding preference of the 4-OH for anomers (figure 8) α-Gal should exhibit higher interlayer and lower intralayer hydrogen bonding than for α-Glc. Again table 1 confirms the expectation.

4.6. *Lyotropic systems*

The internal microseparation surface area as well as the bilayer spacing behave oppositely for α- and β-glycosides (tables 4 and 5). While water addition leads to an increase for β-anomers, α-anomers seem to contract. This behaviour is closely connected to differences in lyotropic LDPs, where β-glycosides show significantly higher separation of bilayer headgroups than do α-anomers. An explanation can be given as follows. β-Glycosides form compact layer structures; the possibility for water to penetrate the layers is low, thus water addition leads to a thin film separating the bilayers. This arrangement naturally drastically reduces interlayer hydrogen bonding between glycolipids, while intralayer hydrogen bonding is only slightly affected. Table 3 confirms this expectation. α-Glycoside-based bilayers, on the other hand, are less compact; because of this, water can be absorbed inside the layers, thus

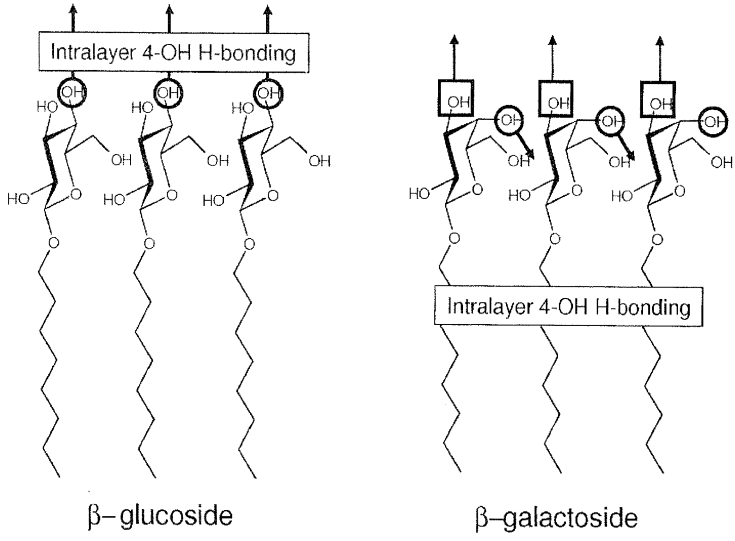

Figure 11. Stereochemical impact on the type of hydrogen bonding. The equatorial OH group in β-C_8Glc favours interlayer H-bonding, while the axial OH group in β-C_8Gal leads to enhanced intralayer H-bonding.

avoiding an expansion of the overall layer spacing. The impact of water on interlayer hydrogen bonding is, as expected, lower than for β-anomers (table 3). Finally the contraction of the bilayers may be explained on the basis of an increase of the overall intralayer cohesion. This force is mediated both by intralayer glycoside interactions and by water-mediated glycoside interactions. An increased intralayer cohesion can lead to a more staggered sugar packing, thus reducing both bilayer spacing and internal surface area. The slightly increased slope for the head group in lyotropic LDPs for α-glycosides (figure 5) is an indication of such a process.

The effect on hydrogen bonding of water addition may also be applied for estimation of water solubilities. Since aqueous solutions of glycosides are based on micelles, intralayer hydrogen bonding is supposedly only slightly affected. Comparing the intralayer hydrogen bonding of octyl β-glucoside and octyl β-galactoside bilayers (β-C_8Glc 2.4 mol^{-1}, β-C_8Gal 2.6 mol^{-1}) with those for the corresponding micelles (β-C_8Glc 0.9 mol^{-1}, β-C_8Gal 1.1 mol^{-1}) [21] we observe a decrease of about 60%. The reduction of hydrogen bonds is to be expected with respect to increased curvature. The constant ratio for hydrogen bonding of the two glycosides in micelle and in bilayer, however, indicates their close relationship. Interlayer hydrogen bonding, on the other hand, is completely eliminated upon forming a solution. Therefore a drastic reduction of interlayer hydrogen bonding upon water treatment should relate to relatively good water solubility. Indeed, as predicted from table 3, the water solubility of β-C_8Glc is remarkably higher than that for α-C_8Glc

5. Conclusions

Computer simulations have proved to be useful tools for the understanding of layer-type assemblies of glycosides. Besides presenting images, they provide characteristic data that can be correlated with experimentally observable physical properties. These correlations lead to an improved understanding of self-assembly and offer predictive tools for new materials. The literature-proposed assumption of increased packing density for the lipophilic region in α-glycosides compared with those in β-anomers [5] could be confirmed. However, this density proved to be a feeble prediction tool, since, despite differences in clearing points for stereomeric glycosides, neither the values for α- nor those for β-glycosides seem to depend on the configuration of the sugar. Varying clearing temperatures for stereoisomeric glycosides can be explained more generally on the basis of differences for the intermolecular hydrogen bonding between glycosides. Quantitative correlations of this hydrogen bonding and the clearing temperature led to reasonable agreement with experimental data. For stereoisomers showing identical values for the total interglycoside hydrogen bonding, intralayer hydrogen bonding can be applied instead, again leading to good agreement with experimental results. This suggests that a major criterion for the stability of layer-structured assemblies of glycosides is the extent of intralayer hydrogen bonding. However, with respect to missing experimental data for two out of six compounds in the investigated series, these conclusions certainly require further evaluation, for example by completing clearing temperature data.

Acknowledgements

We would like to thank the Ministry of Science, Technology and Innovation (MOSTI) for grants 09-02-0309010 SR0004/04 (Glycolipids Science & Technology) and 34-02-03-4001 (E-science GRID) sponsoring this research; Dr Richard Bryce, School of Pharmacy and Pharmaceutical Sciences, University of Manchester, UK and Prof. Vill, University of Hamburg, Germany, for inspiring discussions; the Faculty of Engineering, University of Malaya for providing access to computer facilities, namely the UM Geranium CRAY Cluster; and MIMOS Berhad, Technology Park Malysia for use of the AMD Opteron™ cluster.

References

[1] Anatrace Product Catalog 2002/2003, 6th Edition, pp. 78–79 (2003).
[2] W. Rybinnski, K. Hill. *Angew. Chem. int. Ed.*, **37**, 1328 (1998).
[3] H. Kiwada, H. Niimura, Y. Fujisaki, S. Yamada, Y. Kato. *Chem. Pharm. Bull*, **33**, 753 (1985).
[4] H. Kiwada, I. Nakajima, H. Matsuura, M. Tsuji, K. Yuriko. *Chem. Pharm. Bull.*, **36**, 1841 (1988).
[5] P. Sakya, J.M. Seddon, V. Vill. *Liq. Cryst.*, **23**, 409 (1997).
[6] V. Vill, R. Hashim. *Curr. Opin. colloid interface Sci.*, **7**, 395 (2002).
[7] A.R. van Buuren, H.J.C. Berendsen. *Langmuir*, **10**, 1703 (1994).
[8] S.E. Feller, R.M. Venable, R.W. Pastor. *Langmuir*, **13**, 6555 (1997).
[9] S. Bogusz, R.M. Venable, R.W. Pastor. *J. phys. Chem. B*, **104**, 5462 (2000).
[10] S. Ohta-lino, M. Pasenkiewicz-Gierula, Y. Takaoka, H. Miyagawa, K. Kitamura, A. Kusumi. *Biophys. J.*, **81**, 217 (2001).
[11] S. Abeyguanartne, R. Hashim, V. Vill. *Phys. Rev. E*, **73**, 011916 (2006).
[12] D.A. Case, D.A. Pearlman, J.W. Caldwell, E.T. Cheatham III, J. Wang, W.S. Ross, C. Simmerling, T.

Darden, T. Darden, K.M. Merz, R.V. Stanton, A. Cheng, J.J. Vincent, M. Crowley, V. Tsui, H. Gohlke, R. Radmer, Y. Duan, J. Pitera, I. Massova, G.L. Seibel, U.C. Singh, P. Weiner, P.A. Kollman. *Amber7 Manual* University of California, p. 208 and 224 (2002).
[13] H.A. van Doren, L.M. Wingert. *Mol Cryst. liq. Cryst.*, **198**, 381 (1991).
[14] O. Ivanciuc. *J. chem. Inf. Comput. Sci.*, **36**, 919 (1996).
[15] V. Vill, T. Böcker, J. Thiem, F. Fischer. *Liq. Cryst.*, **8**, 349 (1989).
[16] I.Y. Torshin, I.T. Weber, R.W. Harrison. *Protein Eng.*, **15**, 359 (2002).
[17] V. Vill, H.M. von Minden, M.H.J. Koch, U. Seydel, K. Brandenburg. *Chem. Phys. Lipids*, **104**, 75 (2000).
[18] R. Hashim, H.H. Abdalla Hashim, N.Z. Mohd. Rodzi, R.S. Duali Hussen, T. Heidelberg. *Thin solid Films*, **509**, 27 (2006).
[19] T. Tsuda, R. Arihara, S. Sato, M. Koshiba, S. Nakamura, S. Hashimoto. *Tetrahedron*, **61**, 10719 (2005).
[20] A.A. Gurtovenko, H. Tatra, M. Karttunen, I. Vattulainen. *Biophys. J.*, **86**, 3461; PDB-file www.apmaths.uwo.ca/~mkarttu//downloads (dmpc128_20ns.pdb) (2004).
[21] T.T. Chong, R. Hashim, R.A. Bryce, *J. phys. Chem.* (in the press).